SYNTHESIS, CHARACTERIZATION, ANTIMICROBIAL AND CATALYTIC ACTIVITY OF LIGAND CAPPED COPPER NANOPARTICLES

Varun Kumar Bale, Hussain Reddy Katreddi*

Department of Chemistry, Sri Krishnadevaraya University, Anantapuramu, Andhra Pradesh, India
*Corresponding author: khussainreddy@yahoo.co.in

ABSTRACT

The aim of this research work is to report novel ligand capped copper nanoparticles and their catalytic and antimicrobial activity. In the present investigation, CuNP-L$_1$ and CuNP-L$_2$ were produced by reducing copper sulphate with ligands viz, ascorbic acid and 4-hydroxybenzaldoxime in aqueous medium without inert gas insulation at low temperature (80°C) respectively. The ligand capped copper nanopartices were characterized by UV-Visible and FT-IR spectroscopy, Powder X-ray diffraction (PXRD) and Scanning electron microscopy-energy dispersive spectroscopy (SEM-EDX). From major diffraction peaks, the average particle size was determined using Debye-Scherrer equation. The catalytic activity of capped copper nanoparticles in the reduction of 4-nitrophenol to 4-aminophenol was investigated and compared. Antimicrobial activity of present copper nanoparticles was studied against the pathogens viz. *Staphylococcus aureus*, *Escherichia coli,* and *Candida albicans*.

Keywords: Copper nanoparticles, Ascorbic acid, 4-Hydroxybenzaldoxime, SEM-EDX, PXRD, Catalyst, Antimicrobial activity, 4-nitrophenol.

1. INTRODUCTION

Metal nanoparticles (MNPs) play a significant role in the fields of electronics [1-4], optics [5], heterogeneous catalysis [6-9], agriculture [10], medicine [11] and in biology [12]. MNPs show much attraction during the last decades due to their large surface area, adjustable morphology, and distinctive quantum properties. Among different MNPs, copper nanoparticles (CuNPs) received much attention due to low cost and high abundance compared to noble metals [13-15] like platinum, gold and silver. In general, there are various top-down and bottom-up approach techniques to synthesize the MNPs, they are sol-gel process, lithography, chemical reduction, thermal reduction photolithography, green synthesis, electrochemical, sonochemical process, and electron beam lithography process.

Nano sized metal catalyst provide large surface area than the bulk metal catalyst. MNPs provide high surface for the reactants to interact. CuNPs tend to be unstable and therefore special precautions have to be taken to avoid aggregation and oxidation to air. Various capping agents [16-18] have been used to stabilize and by tuning the reaction conditions, the size of the CuNPs can adjust.

CuNPs are reported to have antimicrobial activity against various bacterial [19-20] and fungal [21] species like *E. coli*, *S. aureus*, *C. albicans* etc. Our recent publications [22, 23] focused on synthesis and characterization of copper nanoparticles. Keeping application aspects of CuNPs in view, the present study focused on catalytic and antimicrobial activity of ligand capped CuNPs besides its synthesis and characterization using UV-Visible and FT-IR spectroscopies, PXRD and SEM-EDX techniques. Two ligands viz. ascorbic acid (L$_1$) and 4-hydroxybenzaldoxime (L$_2$) are used in the preparation of ligand capped nanoparticles, CuNP-L$_1$ and CuNP-L$_2$ respectively. The ligands have been considered as potential reducing and capping agents. Antimicrobial activity of capped nanoparticles against pathogenic bacteria and fungi are uncovered in this work.

4-Nitrophenol (4-NP) is one of the most toxic pollutants in water [24], while 4-aminophenol (4-AP) is less poisonous with many applications such as photographic developer, antioxidant and corrosion inhibitor [25, 26]. Thus, the catalytic reduction of 4-NP to generate 4-AP using capped CuNPs is considered as an important research activity to reduce environmental

pollution. The catalytic activity present capped nanoparticles [CuNP-L_1 and CuNP-L_2] in the reduction 4-NP to 4-AP is delineated in this research article.

2. EXPERIMENTAL

2.1. Material and Reagents

In the present study, all the reagents used were of AR grade and used without any further purification. Copper (II) sulphate pentahydrate, was used as precursor in the preparation of copper nanoparticle. 4-Hydroxy-benzaldoxime ($C_7H_7NO_2$) and ascorbic acid ($C_6H_8O_6$) are used as reducing agents. Ethanol (C_2H_5OH) was distilled before use.

2.2. Synthesis of capped copper nanoparticles (CuNP-L_1) using ascorbic acid

Aqueous $CuSO_4.5H_2O$ solution (0.01M) was taken in a round bottomed flask (250-mL) and heated in a mantle to about 80°C. To this hot solution, Ascorbic acid solution (1g in 25mL deionised water) was added drop wise with continuous magnetic stirring. The reaction

mixture changed colour from blue to green and finally to brownish red which indicates the formation of copper nanoparticles. The mixture was centrifuged at 5000rpm and then separated. It was washed with deionised water and ethanol and finally dried under vacuum.

2.3. Synthesis of capped copper nanoparticles (CuNP-L_2) ligand using 4-Hydroxybenzal doxime

Aqueous $CuSO_4.5H_2O$ solution (0.01M) was taken in a round bottomed flask (250-mL) and heated in a mantle to about 80°C. To this hot solution, 4-hydroxy-benzaldehydoxime (2g in 10 mL of ethanol) was added drop wise with continuous magnetic stirring. The reaction mixture changed colour from blue to green and finally to brownish red which indicates the formation of copper nanoparticles. The mixture was centrifuged at 5000rpm and then separated. It was washed with deionised water and ethanol and finally dried under vacuum. Synthesis of CuNP-L1 and CuNP- L_2 is depicted in Scheme 1.
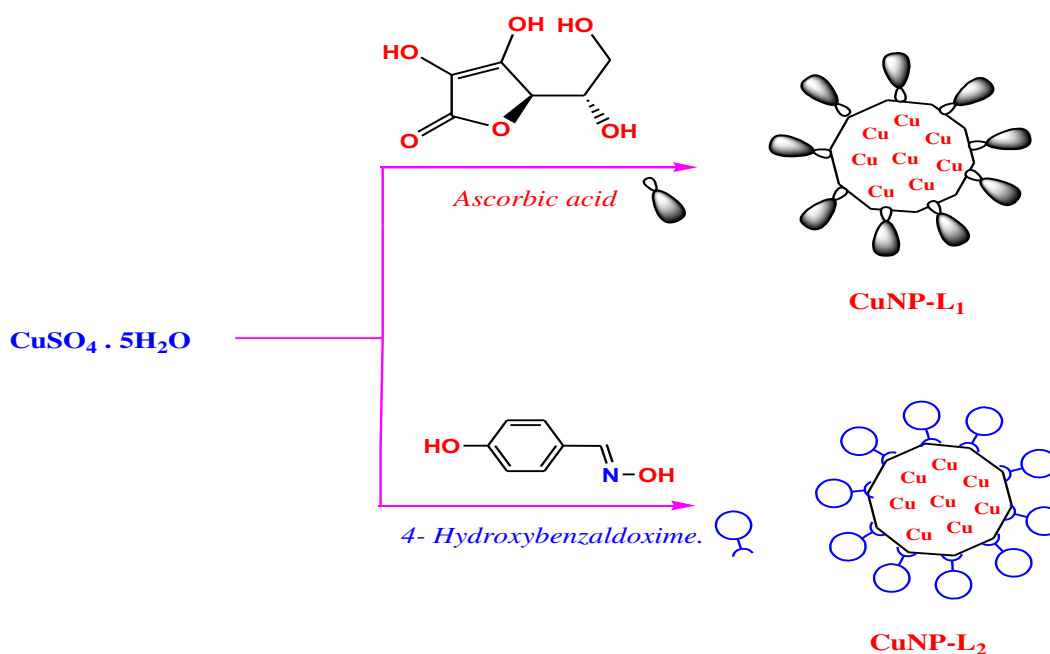
Scheme 1: Schematic representation for syntheses of CuNP-L_1 and CuNP- L_2

2.4. Characterization techniques

ELICO double beam UV-Visible spectrophotometer (SL-210), Perkin Elmer IR spectrophotometer. Powder X-ray spectrometer (Brucker-AXS) and Scanning electron microscopy (SEM, JEOL, IT500 LA), Energy dispersive X-ray spectrometer at an accelerating voltage 20.0kV were used in the present study.

2.5. Antimicrobial activity

The synthesized copper nanoparticles were screened for antimicrobial activity by disc diffusion method against different microorganisms Gram-negative *E. coli;* Gram-positive *S. aureus*, and *C. albicans* fungal species. The sterilized discs were kept in metal nanoparticle dispersion in DMSO in different concentrations (100,

200, 300 and 500 mcg/mL) for 2 hours and then dried in oven at 40°C. The impregnated metal nanoparticle discs were placed on the petri plates and kept for analysis and their zones of inhibition were measured. Standard antibiotics Ciprofloxacin for bacteria and Flucanazole for fungal species were used as reference compounds and 10% dimethyl sulfoxide (DMSO) was used as negative control (blank).

2.6. Catalytic activity

The copper nanoparticles (CuNP-L$_1$ and CuNP-L$_2$) were used as catalyst for the reduction of 4-nitrophenol (4-NP) to 4-aminophenol (4-AP) by sodium borohydride (NaBH$_4$). In quartz 3-mL cuvette 1 mL of 0.2M freshly prepared NaBH$_4$ and 4-nitrophenol (1.9mL, 0.2mM) solution were thoroughly mixed. The

cuvette was then placed in UV-VIS spectrophotometer and spectrum was recorded immediately in the range of 200-800 nm. The spectra were recorded at regular time intervals (5 min) in the range of 200-800 nm after the addition and thorough mixing of 0.10 mL of 1% CuNPs solution.

3. RESULTS AND DISCUSSION
3.1. UV-VISIBLE Spectral Analysis

The UV-Visible spectra of copper nanoparticles recorded in methanol solvent are shown in fig. 1. Spectra indicate that CuNP-L$_1$ and CuNP-L$_2$ show absorption maxima at 351 and 361 nm respectively.

A single isotropic absorption peak in the visible region indicates spherical shape nano particles according to Mie's hypothesis [27].
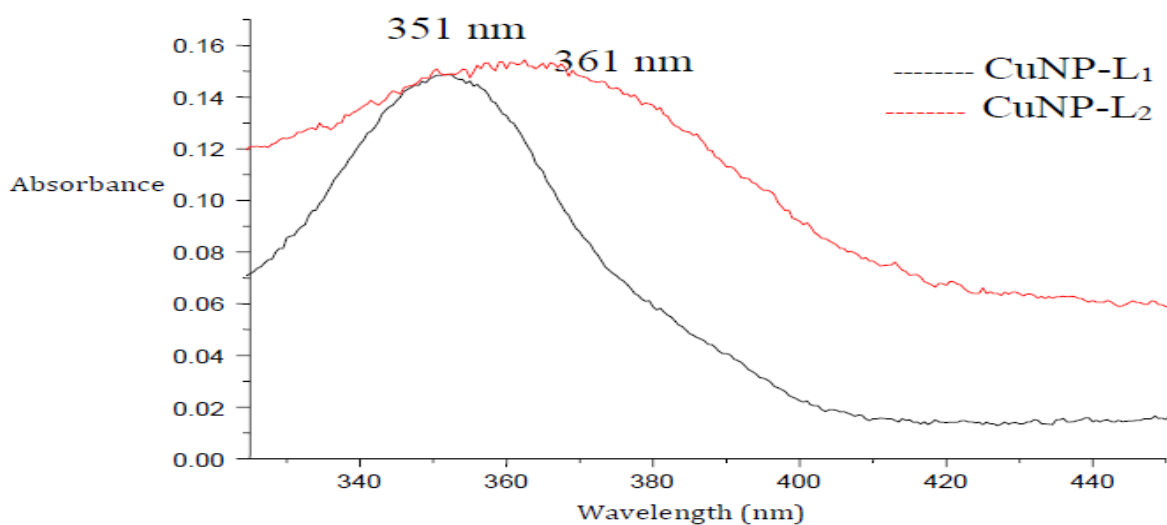
Fig. 1: UV– Visible spectra of CuNP-L$_1$ and CuNP-L$_2$

3.2. FT-IR spectral Analysis

FTIR spectra of CuNPs were recorded in KBr discs in the range of 4000-400 cm^{-1}. FT-IR spectrum of Cu NP-L$_1$ shows bands at 3294 cm^{-1} due to O-H stretching, sharp and intense bands at 1613 cm^{-1}, 1459 cm^{-1}, and 1369 cm^{-1} due to C=C stretching vibration and C-H scissor bending and C-H deformation vibration a band at 1083 cm^{-1} C-O-C stretching vibration respectively. These bands (fig. 2) are due to ascorbic acid ligand that bound to nanoparticle in CuNP-L$_1$.

In the IR spectrum (fig. 3) of CuNP-L$_2$ a medium band is observed at 3400 cm^{-1} which is assigned to O-H stretching vibration of oxime group, Strong band at 1666 , 1610 & 1525 cm^{-1} are respectively assigned to

azomethine (>C=N) and aromatic carbon-carbon stretching vibrations.

A sharp band at 1080 cm^{-1} is due to C-O stretching vibration. The above characteristic bands suggest that the ligand, 4-hydroxybenzaldoxime is binding to the nano-sized particle in CuNP-L$_2$.

3.3. POWDER X-RAY DIFFRACTION Analysis

The powder XRD of copper nanoparticles were recorded between 2θ values 20-80°. The XRD patterns of standard CuNP JCPDS-04-0836 (A), CuNP-L$_1$ and CuNP L$_2$ are depicted in fig. 4.
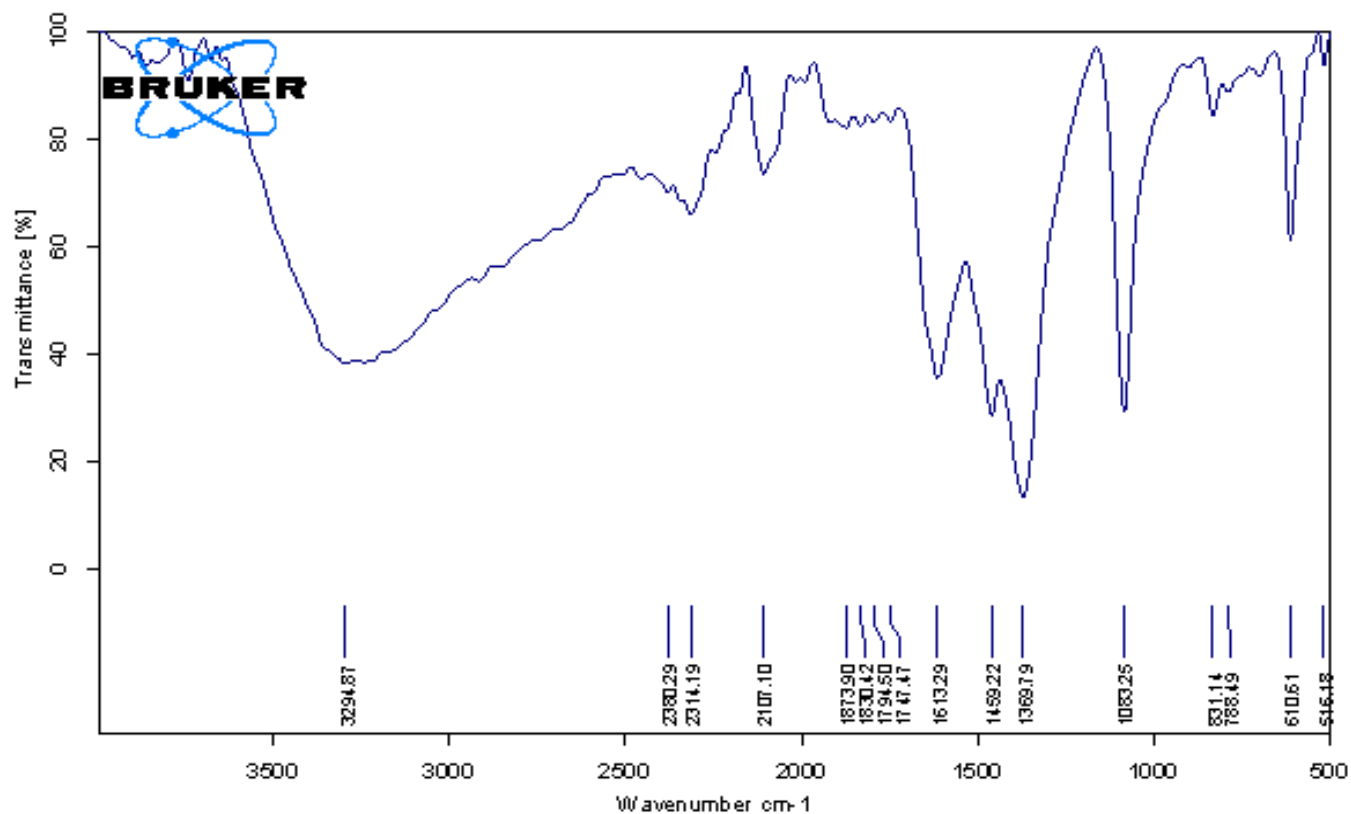
Fig. 2: IR spectrum of CuNP-L$_1$ in KBr medium
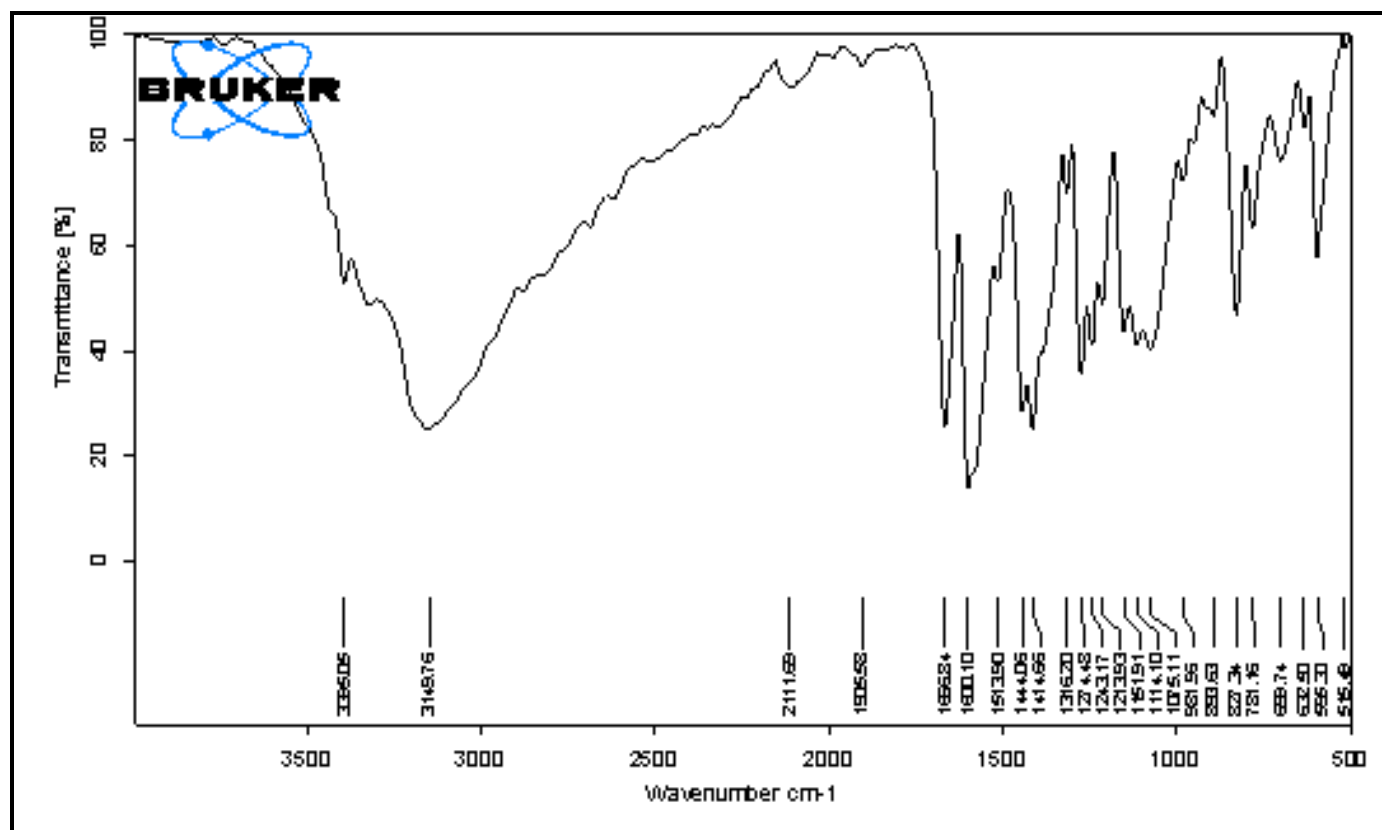
Fig. 3: IR spectrum of CuNP-L$_2$ in KBr medium
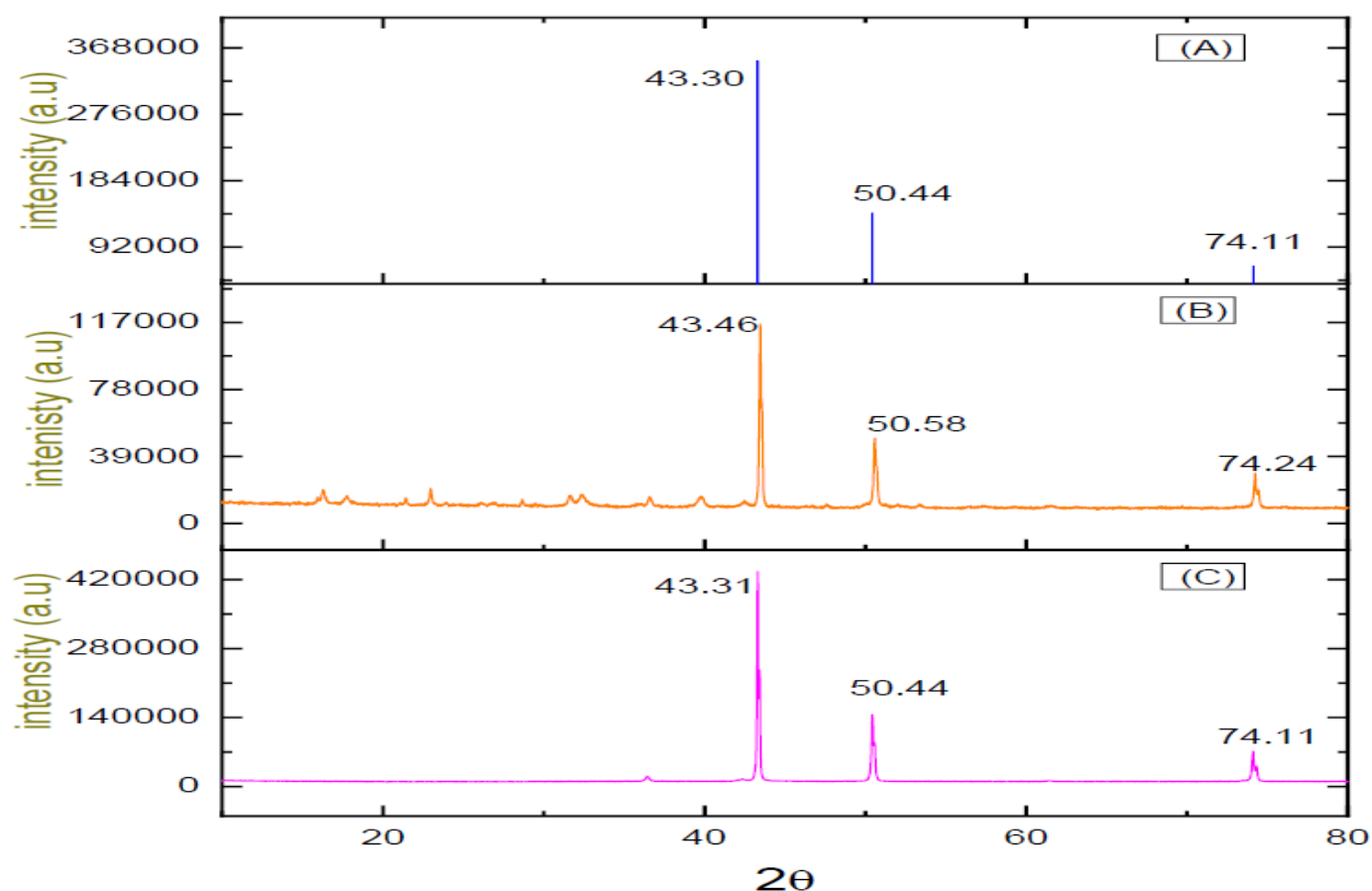
Fig. 4: XRD pattern of (A) CuNP-standard JCPDS-04-0836; (B) CuNP-L₂ and (C) CuNP-L₁

Diffraction peaks of CuNP-L$_1$ (43.31, 50.44, and 74.11) and CuNP-L$_2$ (43.46, 50.58, and 74.24) correspond to h k l indexing (1 1 1), (2 0 0) and (2 1 1) respectively that coincide with standard JCPDS-04-0836 of copper. Thus the diffraction peaks of nano particles related to Face centered cubic phase (FCC). Experimental and standard diffraction angles are given in table 1.

Table 1: Diffraction angles (2θ) values of Copper Nanoparticles

CuNP-L$_1$	CuNP-L$_2$	JCPDS-Cu-04-0836
43.31	43.46	43.30
50.44	50.58	50.44
74.11	74.24	74.11

Particle size calculation: The average particle size of metal nanoparticles were calculated by Debye-Scherer formula [28-30]. The equation is given below.

$$D = 0.9\,\lambda\,/\,\beta\cos\theta$$

Where, λ = x-ray wavelength (0.1541nm); β = Full width half maximum (rad); θ= diffraction angle. On substituting the values and on calculation, the particle size was found to be 40-50 nm for CuNP-L$_1$ and 35-46 nm for CuNP-L$_2$.

3.4. Scanning electron microscopy and energy dispersive X-ray spectroscopy analysis

The surface morphology and size of copper nanoparticles were uncovered using Scanning Electron Microscopy (SEM). The SEM micrograph (fig. 5) CuNP-L$_1$ suggested that the particles have spherical morphology with agglomeration. The particles size is in the range 40-55 nm.

Fig. 6 shows SEM micrographs of CuNP-L$_2$. Its particle size is in the range, 35-45 nm. The results indicate that the capping agent, 4-hydroxybenzaldoxime effectively controls the size of nano particle.

EDX analysis shows the elemental constitution of synthesised copper nanoparticles. The EDX spectrum of CuNP-L$_1$ is manifested in fig. 7. It confirms the existence of Cu, C and O and traces of Si and S were observed. The weight percentages of Cu, C, O, Si, and S from analysis are given in table 2. The EDX spectrum

of CuNP-L$_2$ is manifested in fig. 8, which confirms the existence of Cu, C, O, N, and traces like S, Cl were also observed. The weight percentages of Cu, C, O, N, S, and Cl from analysis are included in table 2.
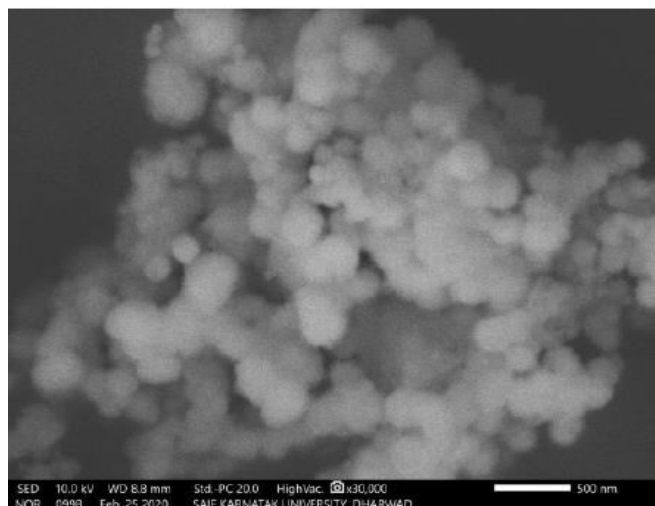
Fig. 5: SEM micrographs of CuNP-L$_1$
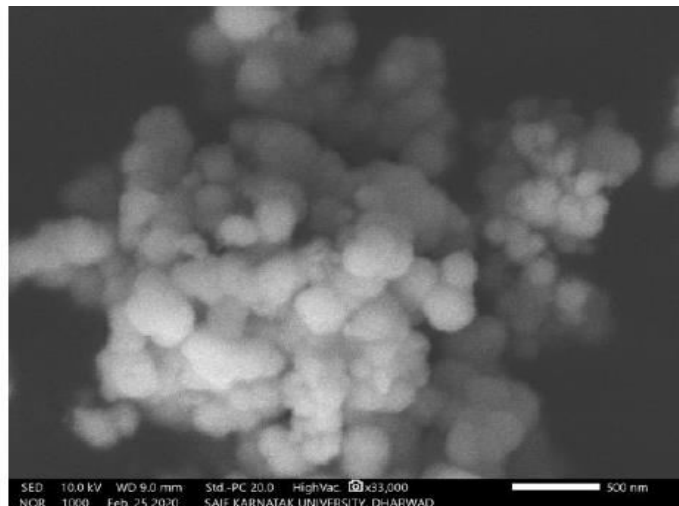
Fig. 6: SEM micrographs of CuNP-L$_2$
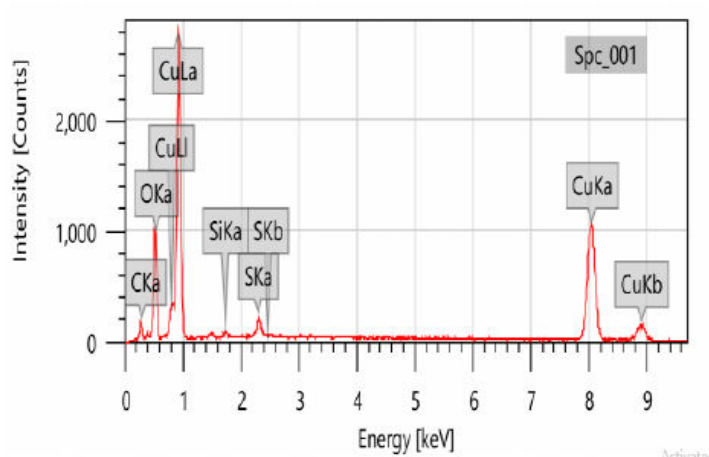
Fig. 7: EDX spectrum of CuNP- L$_1$
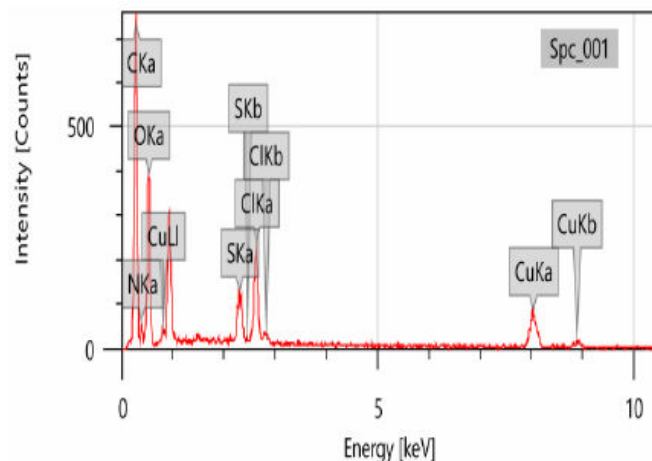
Fig. 8: EDX spectrum of CuNP- L$_2$

Table 2: Percentage of elements in CuNP-L$_1$ and CuNP-L$_2$

Element (Wt%)	Cu	C	O	Si	N	S	Cl
CuNP-L$_1$	35.68	21.77	40.27	0.6	-	1.68	-
CuNP-L$_2$	37.72	24.97	19.08	-	13.86	1.41	2.95

In fig.7, the EDX spectrum, the peak at 0.5 keV relates to binding energy of Oxygen (OK$_\alpha$) and a peak at 0.27 is due to Carbon (CK$_\alpha$). The peaks at 2.34, 2.48 relates to Sulphur (SK$_\alpha$ & SK$_\beta$) and peaks at 2.67 and 2.91 relates to Chlorine (ClKα & ClK$_\beta$). The crests at 0.84; 0.94; 8.04 and 8.94 keV are assigned to CuL$_1$, CuL$_2$, CuK$_\alpha$, and CuK$_\beta$.

In fig. 8, the EDX spectrum, the peak at 0.5 keV relates to binding energy of Oxygen (OK$_\alpha$), a peak at 0.27 is due to Carbon (CK$_\alpha$), a peak at 0.78 is due to Nitrogen (NK$_\alpha$), peak at 2.34, 2.48 relates to Sulphur (SK$_\alpha$ & SK$_\beta$) and peak at 1.78 relates to Silicon (SiK$_\alpha$). The crests at 0.84; 8.04 and 8.94 keV are assigned to CuL$_1$, CuK$_\alpha$, and CuK$_\beta$ respectively.

3.5. Antimicrobial activity

The antimicrobial activity of CuNP-L$_1$ and CuNP-L$_2$ were screened against the bacteria Gram-positive

Staphylococcus aureus, Gram-negative *Escherichia coli* and fungal species *Candida albicans* by using Agar disc diffusion method. Nutrient agar medium was taken in petri-plates and solidified. About 6 mm discs are soaked in standard references positive controls (viz. ciprofloxacin for bacteria and flucanazole for fungi) and in different concentrations of metal nanoparticles dispersed in DMSO. A 10% DMSO was taken as negative control (Blank). Photographs of discs showing

inhibition zones are shown in fig. 9. The zone of inhibition values are given in table 3.

Data revealed that the zone of inhibition increases with increase in concentration of copper nanoparticles. CuNP-L_1 and CuNP-L_2 showed nearly similar antibacterial and antifungal activity. The graphical representation of anti-microbial activity of nano particles is shown in fig. 10.

(A) **(B)**
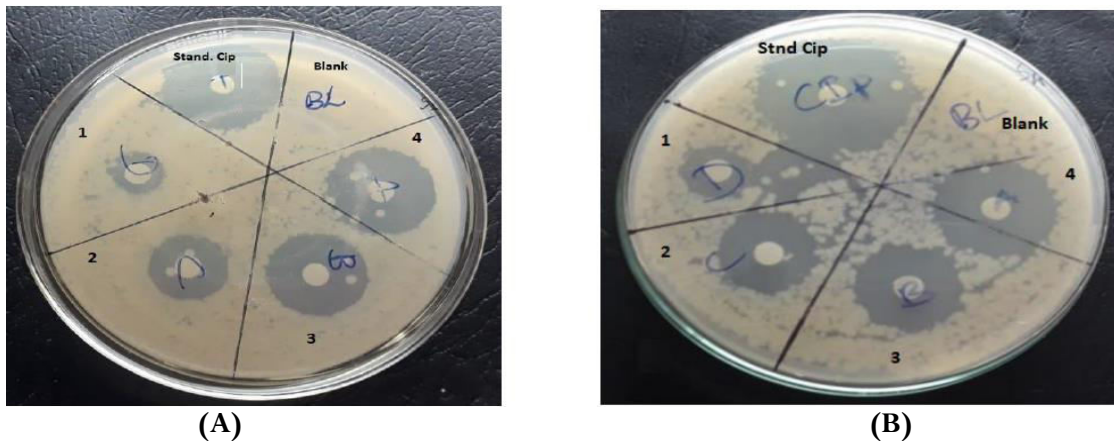
Cip means Ciprofloxacin:CuNP concentration 1- 100 mcg, 2- 200 mcg, 3- 300 mcg, 4- 500 mcg and Blank with (10% DMSO).

Fig. 9: Photographs showing inhibition zones for bacteria *S. aureus* A) for CuNP-L_1 and (B) for CuNP-L_2
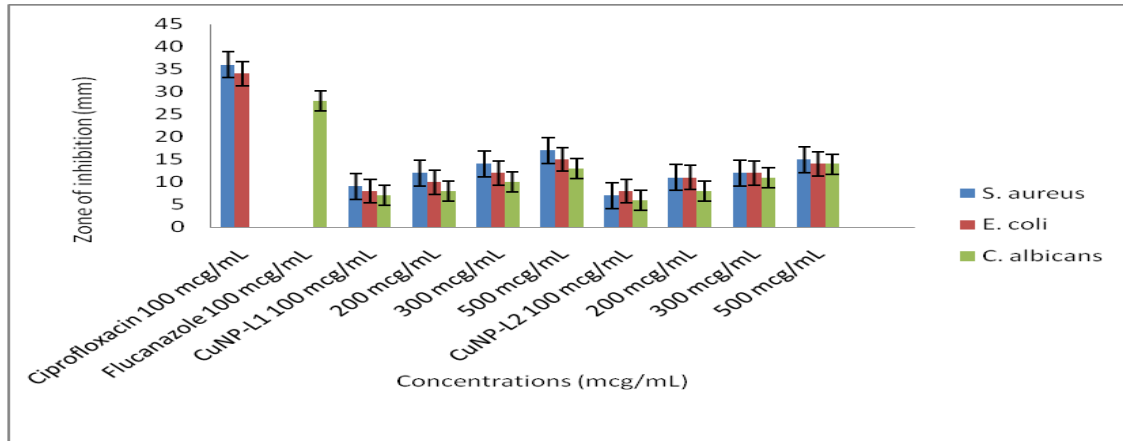
Fig. 10: Bar graph representing antimicrobial activity of copper nano particles

Table 3: Antimicrobial activity of copper nanoparticles against pathogens

Samples	Treatment (mcg/mL)	*S aureus*	*E coli*	*C albicans*
Standard Ciprofloxacin	100	36	34	-
Standard Flucanazole	100	-	-	28
CuNP-L_1	100	9	8	7
	200	12	10	8
	300	14	12	10
	500	17	15	13
CuNP-L_2	100	7	8	6
	200	11	11	8
	300	12	12	11
	500	15	14	14

3.6. Catalytic activity

UV-Visible spectra of 4-nitrophenol (4-NP) in the presence and in absence of $NaBH_4$ are shown in fig. 11. The 4-NP in the absence of $NaBH_4$ shows absorption maximum at 317 nm. But in the presence of $NaBH_4$, the absorption maximum is shifted to 400 nm.

Spectra of reaction mixture in the cuvette were recorded at different time intervals after the addition of 0.10 mL of 1% CuNP-L_1 solution. Spectra indicated that intensity of peak at 400 nm decreases with time and a new peak is observed at 290 nm at 25 min due to the conversion of 4-nitrophenol (4-NP) to 4-aminophenol (4-AP). Similar trend was observed (fig.12) even with CuNP-L_2.

(A)

(B)
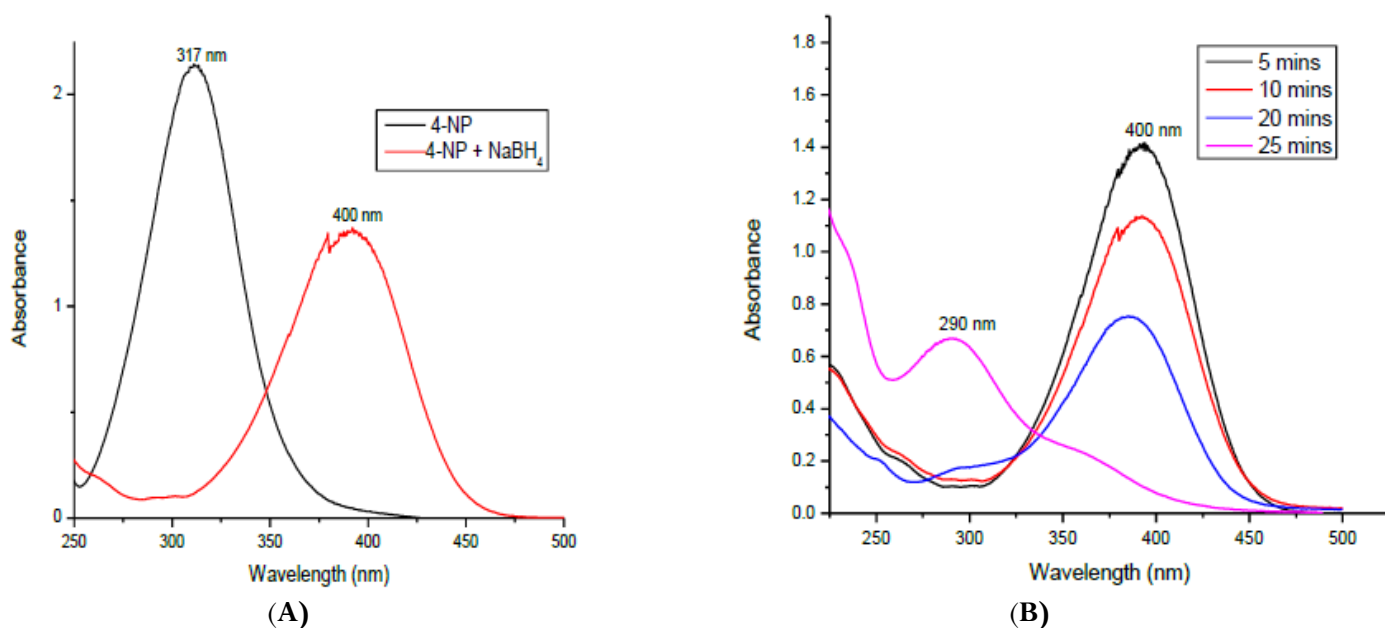
Fig. 11: A) Absorption spectra of 4-Nitrophenol (4-NP) in the absence and in the presence of $NaBH_4$ B) Absorption spectra of reaction mixture containing 4-NP, $NaBH_4$ and CuNP-L_1 at different time intervals.
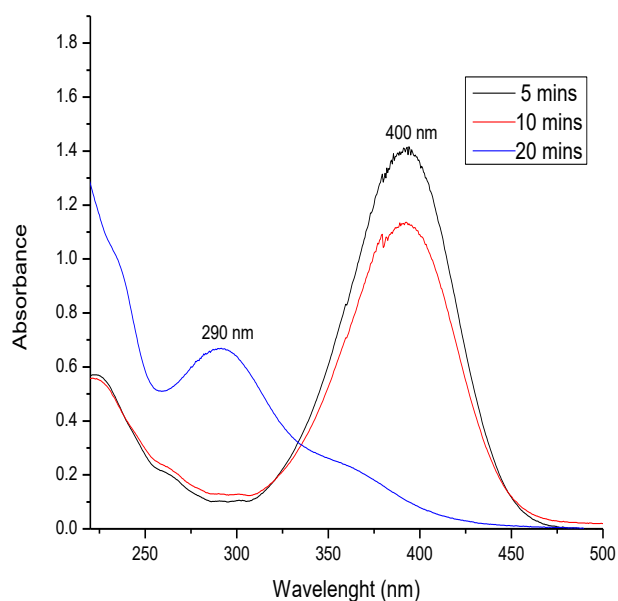
Fig. 12: Absorption spectra of reaction mixture containing 4-NP, $NaBH_4$ and CuNP-L_2 at different time intervals

3.7. Characteristics of 4-NP reduction using capped copper nanoparticles

The ultra violet-visible (UV-Vis) spectrum of the 4-NP in water was recorded. It has been observed that a red shift of the peak due to 4-NP from 317 to 400 nm occurred immediately after the addition of $NaBH_4$. This is because of the formation of 4-nitrosophenol caused by $NaBH_4$. In the absence of any catalyst, the peak at 400 nm remained unaltered even for a couple of days. Addition and proper mixing of an aliquot of copper nanoparticles (CuNP-L_1 or CuNP-L_2) to the reaction mixture caused the fading and ultimate bleaching of the yellow colour of the 4-NP solution. This discoloration was quantitatively monitored spectrophotometrically with time and has been noted as a successive decrease of the peak height. This was due to the reduction of 4-NP to 4-AP. When the colour was completely discharged, i.e. after the completion of the reduction, a new peak appeared at 388 nm due to Copper Plasmon absorption. The successive decrease in the intensity and concomitant blue shift of the peak from 400 to 290 nm (fig. 11) was

observed during the course of reaction. In the intermediate stage of reduction, the peak due to the Cu Plasmon band could not be observed which remained masked within the absorption band of the nitro compounds but finally a clear absorption band at 290 nm due to Cu plasmon band appeared. In another way, the reduction can be visualized by the disappearance of the 400 nm peak with the concomitant appearance of a new peak at 290 nm. It can be said clearly that the peak at 290 nm is due to 4-AP because the same peak could be observed for an authentic 4-AP solution under identical experimental conditions where reduction of 4-NP is carried out in the presence of CuNPs. The reduction mechanism of 4-NP to 4-AP is shown in Scheme 2.

Reduction of 4-NP to 4-AP is thermodynamically favourable (E_0 = -0.76 V Vs NHE) and H_3BO_3/BH_4^- (E_0 = -1.33 V Vs NHE) produced a large potential difference (large energy gap) between 4-NP & BH_4^- makes the reaction kinetics slower.

The added copper nanoparticles adsorb electrons (negative ions) and able to transfer electrons donated by borohydride ions to nitro group of 4-NP, which is expected to decrease the kinetic barrier and thus catalyse the reduction reaction. A complete disappearance of peak at 400nm takes 25 minutes for CuNP-L_1 and where as for CuNP-L_2 takes 20 minutes. The rate constant is calculated with the equation ln $[A]/[A_0]$ = - k t. where [A] concentration at time 't' $[A_0]$ is the initial concentration, and k is rate constant. The rate constant for CuNP-L_1 is 4.25×10^{-2} min^{-1} where as for CuNP-L_2 is 4.67×10^{-2} min^{-1}.

(A) 4-Nitrophenol, (B) 4-Nitrosophenol, (C) 4-Hydroxylamino phenol and (D) 4-Aminophenol

Scheme 2: **Mechanism for the reduction of 4- NP to 4 -AP**

4. CONCLUSION

Novel ligand capped copper nanoparticles are synthesized and their morphology and sizes are characterized on the basis of UV-Visible and IR spectroscopies and Powder XRD and SEM- EDX analysis. The ligand capping is evidenced by IR spectroscopy. Antimicrobial and catalytic activity of CuNPs are investigated in the present research work. Ligand capped copper particles (CuNPs) having low particle size (35-30 nm) are investigated for the first time. The nano-sized particles showed significant catalytic and antimicrobial activity. The present CuNPs maybe routinely used as catalysts in the reduction of toxic 4-nitrophenol to harmless and useful 4-aminophenol. The authors are planning to study metal nanoparticles capped with coordination compounds possessing catalytic and antimicrobial activity.

Conflict of interest
The authors declare that there is no conflict of interest regarding the publication of this article.

6. REFERENCES

1. Volkman SK, Pei Y, Redinger D, Yin S, Subramania V. *Mater. Res. Soc. Symp. Proc.*, 2004; **814**:17.8.1-17.8.4.
2. Park BK, Kim D, Jeong S, Moon J, Kim JS. *Thin Solid Films*, 2007; **515**:7706-7711.
3. Woo K, Kim D, Kim JS, Lim S, Moon J. *Langmuir*, 2009; **25**:429-433.
4. Lee Y, Choi JR, LEE KR, Stott NE, Kim D. *Nanotechnology*, 2008; **19**:415604.

5. Jang S, Seo Y, Choi J, Kim T, Cho J, Kim S, Kim D. *Scripta Mater.*, 2010; **62**:258-261.

6. Singh P, Katyal A, Kalra R, Chandra R. *Tetrahedron lett*, 2008; **49**:727-730.

7. Wei X, Zhu B, Xu Y. *Colloid Polym. Sci.,* 2005; **284**:102.

8. Grouchko M, Kamyshny A, Ben-Ami K, MAgdassi S. *J. Nanopart. Res.*, 2009; **11**:713-716.

9. Dang TMD, Nguyen TMH, Nguyen HP. *Adv. Nat. Sci.:Nanosci. Nanotechnol.,* 2010; **1**:025011.

10. Deepti M, Gurjeet K, Singh P, Yadav K, Azmal Ali. *Front. Nanotech*, 2020; **02**:04 December.

11. Abdulla-Al-Mamun M, Kusumoto Y, Muruganandham M. *Mater Lett.*, 2009; **63**:2007-2009.

12. Kumar SA, Cheng HW, Chen SM, Wang SF. *Mater Sci. Eng.*, 2010; **30**:86-91.

13. Khanna PK, Gaikwad S, Adhyapak PV, Singh N, Marimuthu R. *Mater. Lett.,* 2007; **61**:4711-4714.

14. Luo N, Liu KX, Li XJ, Wu ZW, Wu SY, Ye LM, Shen Y. *Mendeleev Commun.*, 2012; **22**:1-3.

15. Seo JY, Kang HW, Jung DS, Lee HM, Park SB. *Mater. Res. Bull.*, 2013; **48**:1484-1489.

16. Javed R, Usman M, Tabassum S, Zia M. *Appl Surf. Sci.* 2016; **386**:319-26

17. Niu Z, Li Y, *Chem Mater.* 2014; **26**:72-83.

18. Wu C, Mosher BP, Zeng T. *Mater. Res. Soc. Symp. Proc.*, 2005; **879**:E Z6.3.1

19. Chandraleka S, Ramya K, Chandramohan G, Dhanasekaran D, Priyadharshini A, Panneerselvam A. *J. Saudi. Chem. Soc,.* 2014; **18**:953-962.

20. O'Gorman J, Humphreys H. *J. Hosp. Infect.,* 2012; **8**:217-223.

21. Gordon AS, Howell LD, Harwood V. *Can. J. Microbiol.,* 1994; **40**; 408-411.

22. Varun Kumar B, Parveen Taj Y, Hussain Reddy K. *Asian Journal of Chemistry*, 2020; **32**:2130-2134.

23. Murali Krishna P, Hussain Reddy K, Rashmitha N, Shravanthi M, Sujathamm D. *Asian Journal of Chemistry,* 2020; **32**:2700-2706.

24. Guo M, He J, Li Y, Ma S, Sun X. *J Hazard Mater.*, 2016; **310**:89.

25. Wang L, Yang Q, Cui Y, Gao D, Kang J, Sun H, Zhu L, Chen S. *New J Chem.,* 2017; **41:**8399.

26. Zhang J, Chen G, Guay D, Chaker M, Ma D. *Nanoscale,* 2014; **6**:2125.

27. Mie G. *Ann. Phys.,* 1908; **330**:377.

28. Champion Y, Bigot J. *Mater. Sci. Eng. A*, 1996; **58**:217-218.

29. Girardin D, Maurer M. *Mater. Res. Bull.,* **25**:119-127.

30. Boulaud D, Chouard JC, Briand A, Chartier F, Lacour L, Mauchien P, Mermet JM. *J. Aerosol Sci.,* 1992; **23**:225-228.